ISSN: 2720-989X
JEEE
JOURNAL OF ENERGY AND ELECTRICAL ENGINEERING

Observability-Aware Mobility Parameter Estimation for Seamless Indoor-Outdoor Vehicle Positioning

Md Emadur Rahman Ekra[1], Md Nadim Hosain[2], Md Daud Ibrahim[3], Md Imran Hossain[4], Md Belayet Hossain Babla[5]
[1,2,3,4,5] School of Electronic and Information Engineering, Nanjing University of Information Science & Technology, Nanjing, China
[1] email: mdemandekra@nuist.edu.cn

[*submitted*: 04-04-2026 | *review*: 11-04-2026 | *published*: 30-04-2026]

ABSTRACT: *Seamless indoor-outdoor positioning remains challenging due to heterogeneous sensing, multipath and attenuation indoors, and time-varying GNSS quality outdoors. This paper presents a simulation-based framework for mobility parameter estimation of a four-wheel vehicle transitioning from an indoor environment (Building A) through an outdoor segment and into a second indoor environment (Building B). The proposed system fuses GNSS (GPS/SBAS), BLE received signal strength (RSS), IMU, and odometry using a nonlinear state-space vehicle model. This study implements and compares the Extended Kalman Filter (EKF), Unscented Kalman Filter (UKF), Particle Filter (PF), and an Interactive Multiple-Model EKF (IMM-EKF) that combines rectilinear and curvilinear motion models. In addition, this work examines state observability under different sensor-availability conditions using an EKF-based local linearization approach. Simulation results show that multi-sensor fusion improves trajectory estimation under noisy observations; in the tested scenario, IMM-EKF achieves the most consistent overall performance (e.g.,* $\sigma_x = 2.51$ *m,* $\sigma_y = 3.11$ *m). Observability analysis indicates full observability when IMU is available (rank* $= 7$*), while GPS-only and odometer-only configurations are not fully observable. These findings support more robust indoor-outdoor positioning by combining heterogeneous sensing with nonlinear filtering and observability-aware analysis.*

KEYWORDS: *Mobility parameter estimation; Indoor-outdoor positioning; Heterogeneous sensor fusion; IMM-EKF; Observability analysis.*

I. INTRODUCTION

Location-based services (LBS) have become a core enabling technology for smart buildings, logistics, healthcare, and intelligent transportation, where reliable positioning supports tasks such as asset tracking, safety monitoring, navigation, and automation [1]. However, delivering continuous positioning across indoor and outdoor environments remains difficult because sensing conditions and dominant error sources change abruptly at building boundaries [2]. Outdoor positioning is typically dominated by Global Navigation Satellite Systems (GNSS), while indoor positioning must rely on short-range radio and onboard sensors. This indoor-outdoor heterogeneity creates a practical gap: systems that perform well outdoors often degrade indoors, and purely indoor approaches struggle to remain stable when transitioning to outdoor spaces and back again [2]–[4].

A major technical reason for this gap is that measurement quality is not stationary. Indoors, radio signals can suffer from attenuation, multipath, and obstruction, which causes strong variability in received signal strength (RSS) and other ranging proxies [5]. Bluetooth Low Energy (BLE) beacon systems, for example, are attractive due to low cost and easy deployment, but RSSI-derived distance estimates are often degraded by multipath and fading, making robust modeling and filtering essential [6]. Recent BLE research continues to focus on mitigating RSS variability and improving practical accuracy, including refined BLE distance/position estimation pipelines and fusion with other sensors [7]. At the same time, inertial sensors and odometry provide short-term motion consistency but accumulate drift over time; consequently, recent surveys and studies consistently conclude that multi-sensor fusion is necessary to obtain dependable indoor positioning performance rather than relying on a single modality [8].

For mobile platforms, particularly wheeled vehicles, positioning is fundamentally a mobility parameter estimation problem: estimating position, orientation, and their derivatives from noisy and intermittent measurements [9]. This estimation problem is naturally expressed in a state-space form, but real vehicle motion and heterogeneous measurements are nonlinear, motivating nonlinear filtering and probabilistic inference [10]. The literature increasingly combines complementary sensors (e.g., GNSS, IMU, odometry, BLE/UWB, LiDAR/camera) using filtering and smoothing frameworks [11]. Classical nonlinear Bayesian filters such as the Extended Kalman Filter (EKF), Unscented Kalman Filter (UKF), and Particle Filter (PF) remain widely used due to their practical efficiency and interpretability [12]–[14]; meanwhile, newer tightly coupled formulations and factor-graph approaches improve robustness by better handling

measurement outliers and variable GNSS reliability in difficult environments such as urban canyons [15]. These developments align with the core challenge addressed in this work: maintaining stable, accurate estimation when sensor quality changes across indoor-outdoor transitions.

An additional but often decisive requirement for stable fusion is observability: whether the available measurements contain enough information to recover the full system state [16]. In real deployments, sensors can disappear temporarily (e.g., GNSS blockage near tall buildings), and even short gaps can destabilize Kalman-type fusion if the filter becomes poorly conditioned [17]. Recent work on nonlinear systems continues to expand observability analysis tools and emphasizes that observability is not merely theoretical; it can guide estimator design, sensor selection, and trajectory/sensing strategies [18]. In the context of indoor-outdoor vehicle positioning, understanding which sensor combinations preserve observability is essential to avoiding filter detuning and to designing mitigation strategies when measurements are lost and later recovered [19].

This paper develops and evaluates a simulation-based framework for seamless indoor-outdoor positioning of a four-wheel vehicle using heterogeneous sensors. Following the system assumptions in this study, the proposed pipeline integrates GNSS/GPS with variable quality, BLE RSS measurements, Inertial Measurement Unit (IMU), and odometry within a nonlinear vehicle motion model. This work implements and compares EKF, UKF, and PF, and additionally employs an Interactive Multiple-Model EKF (IMM-EKF) that runs two EKFs in parallel-one matched to rectilinear motion and one matched to curvilinear motion-allowing the estimator to adapt when the vehicle dynamics change. Beyond accuracy comparison, this paper explicitly analyzes state observability under different sensor-availability conditions, highlighting which sensing configurations preserve full observability and how estimator stability can be maintained during intermittent measurement loss (e.g., by retaining filter outputs for correction when measurements return).

The main contributions of this work are:

1) A unified indoor-outdoor positioning framework for wheeled vehicles that fuses GNSS, BLE, IMU, and odometry within a nonlinear state-space model.
2) A comparative evaluation of EKF, UKF, PF, and IMM-EKF under indoor-outdoor transitions and degraded GNSS conditions.
3) An observability-focused analysis of the fused system under different sensor subsets, clarifying the conditions under which reliable mobility parameter estimation is achievable.

Together, these elements provide a structured and practical contribution to robust mobility parameter estimation for seamless indoor-outdoor positioning, with emphasis on implementable filtering methods and system-level observability considerations.

II. RELATED WORK

Seamless indoor-outdoor positioning remains challenging because the sensing conditions and dominant error sources change sharply across buildings, transition zones, and outdoor corridors [20]. GNSS-based positioning is generally reliable under open-sky conditions but degrades in dense urban areas and typically fails indoors, whereas indoor wireless techniques (e.g., BLE, Wi-Fi, UWB) are strongly affected by attenuation, multipath, and non-line-of-sight propagation. As a result, the same sensing modality can exhibit substantially different error behavior across environments, and practical systems must explicitly handle time-varying measurement quality and intermittent availability of key signals (e.g., GNSS outages near tall structures) [21].

Among low-cost indoor technologies, BLE has received sustained attention because of its low power consumption, low cost, and ease of deployment. However, RSSI-based BLE positioning is well known to be sensitive to channel fading, device diversity, and environmental dynamics (e.g., moving objects and layout changes), which can introduce bias and high variance in RSSI-derived distance proxies [22]. Consequently, recent BLE-focused studies emphasize robust modeling and estimation strategies-rather than direct RSSI-to-distance conversion-as well as fusion with complementary sensors to improve stability and accuracy under realistic indoor conditions [23].

Reflecting these limitations, a major trend in recent positioning research is the shift from single-sensor methods to heterogeneous sensor fusion, in which complementary sensors compensate for one another's weaknesses. Survey papers and comparative studies consistently report that combining radio measurements with motion sensors (e.g., IMU and odometry) improves robustness compared with using wireless or inertial sources alone, particularly in complex indoor environments where signal conditions are highly variable [24]. In many practical pipelines, inertial and odometric sensors provide short-term motion consistency, while radio measurements provide periodic corrections that reduce accumulated drift.

Particle-filter-based fusion is frequently adopted in this context because it can represent non-Gaussian uncertainty and maintain multiple hypotheses when measurements are ambiguous or irregular [25].

A second active direction focuses on transition handling between indoor and outdoor regimes. Instead of switching abruptly between separate indoor and outdoor engines, recent methods aim to detect indoor, outdoor, and transition zones using probabilistic logic and multi-source indicators (e.g., Wi-Fi/BLE RSS patterns combined with GNSS quality measures) [26]. These transition-aware designs are intended to reduce discontinuities at entrances, improve temporal continuity, and stabilize estimation during periods of changing measurement reliability [27]. This direction aligns with the scenario considered in this study, where a wheeled vehicle moves between buildings through an outdoor segment with potentially degraded GNSS.

From an estimation viewpoint, indoor-outdoor positioning for mobile platforms is naturally framed as mobility parameter estimation using a (typically nonlinear) state-space model, since vehicle dynamics and sensor measurement relationships are rarely linear over a full trajectory [28]. For this reason, nonlinear Bayesian filtering remains widely used in applied positioning systems [29]. The EKF is popular due to its computational efficiency and mature implementation practices; the UKF is often preferred when linearization error becomes significant; and the PF is commonly used when uncertainty is non-Gaussian, multi-modal, or affected by strong outliers [29]–[31]. In parallel, more recent navigation systems increasingly adopt tightly coupled fusion and smoothing formulations (including factor-graph-based methods) to improve robustness under outliers and variable GNSS quality, especially in challenging environments such as urban canyons [32]. At the same time, interacting and multi-model filtering strategies (e.g., IMM-style designs) have attracted renewed interest for handling changing motion regimes and time-varying sensor reliability, rather than assuming a single motion model is optimal for the entire trajectory [33].

A further factor that directly affects estimator reliability, particularly during measurement loss, is observability, i.e., whether the available measurements contain sufficient information to recover the full system state [34]. In indoor-outdoor operation, sensors often run at different sampling rates and key measurements may temporarily disappear (e.g., GNSS blockage). Under partial sensing, an estimator may become poorly conditioned or drift if the remaining measurements do not preserve observability [35]. Recent work increasingly links observability not only to theoretical identifiability but also to practical filter behavior, sensor selection, and trajectory and sensing strategy, reinforcing the role of observability analysis as a design and validation tool for robust fusion pipelines.

Motivated by these developments, this paper follows the dominant direction of current research-heterogeneous sensor fusion with nonlinear filtering-but focuses specifically on mobility parameter estimation for a four-wheel vehicle undergoing indoor-outdoor transitions using GNSS, BLE, IMU, and odometry, while explicitly assessing observability under partial sensing. This study implements EKF, UKF, and PF baselines and employs an IMM-EKF with separate rectilinear and curvilinear models to better represent changes in vehicle maneuvering. The framework is evaluated in a transition scenario with variable GNSS quality and indoor BLE sensing, and observability rank results are used to interpret which sensor subsets support full-state estimation during measurement loss-an aspect that is widely recognized as important but is not always reported in comparative indoor-outdoor fusion studies.

III. SYSTEM MODEL AND METHODOLOGY

A. PROBLEM DEFINITION AND OVERVIEW

This study focuses on mobility parameter estimation for seamless indoor-outdoor positioning of a four-wheel vehicle. Here, mobility parameter estimation refers to estimating the vehicle's position, orientation, and related motion quantities for an object that may be moving, using information provided by sensors. Fig 1 presents the conceptual framework of mobility parameter estimation based on the comparison between actual vehicle motion and the nonlinear vehicle model. Wireless positioning methods are commonly grouped by the radio characteristics and measured parameters used to determine position [36].

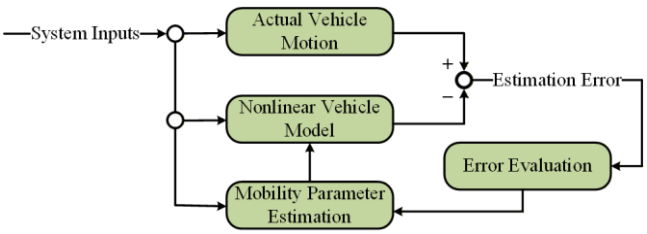

Fig 1. Conceptual Framework of Mobility Parameter Estimation for Nonlinear Vehicle Motion

A widely used motion-based approach is Dead Reckoning (DR), which computes displacement using odometer and inertial sensors such as encoders/tachometers, accelerometers, gyroscopes, and magnetometers. For walking applications, the corresponding approach is known as Pedestrian Dead

Reckoning (PDR) [37]. In indoor environments, fingerprinting is also common; it does not require explicit distance measurement and can provide good accuracy, although performance can drop in highly dense areas and the algorithms can become more complex due to interference-driven variability in RSSI measurements [38]. In addition, indoor positioning can be supported by technologies such as Ultra-Wideband (UWB), and some systems estimate distances from signal strength indicators together with inertial information, using nonlinear filtering (e.g., EKF) to determine coordinates [39].

Because indoor-outdoor transitions introduce changes in measurement quality and availability (for example, noisy GNSS outdoors and limited GNSS indoors), this work adopts a heterogeneous sensor fusion approach. In the considered scenario, the framework integrates GNSS/GPS, BLE, and inertial and odometric sensors to estimate mobility parameters for a vehicle moving between buildings through an outdoor segment. The estimation is performed using nonlinear filtering methods, and the overall methodology compares the EKF, UKF, and PF, including an IMM-EKF designed to handle different motion regimes (straight and curved maneuvering).

B. SENSOR FUSION FRAMEWORK AND STATE-SPACE FORMULATION

Sensor measurements are affected by practical factors such as sensor quality, integrity, sampling frequency, and resolution. As a result, the measured output differs from the ideal physical value by a noise term, which reflects unavoidable uncertainty and imperfections introduced during the sensing and data acquisition process. In this study, the output of sensor i, denoted z_i, is modeled as:

$$z_i = \hat{z}_i + \eta_i \quad (1)$$

where z_i denotes the actual measurement provided by the i-th sensor, while $\hat{z}_i$ is the ideal (true) noise-free value of the same physical quantity and η_i represents the measurement error introduced by sensor uncertainty, environmental interference, finite resolution, and sampling limitations.

To fuse measurements from multiple sensors, the system is expressed in state-space form to provide a unified mathematical representation. For linear dynamics, the standard model is commonly written as follows:

$$\begin{aligned} x_{k+1} &= Ax_k + w_k \\ z_k &= Hx_k + \eta_k \end{aligned} \quad (2)$$

where x_k is the state vector, A is the state transition matrix, H maps the state to the observation space, and w_k and η_k represent process noise and measurement noise, respectively. Given an observation z_k, the estimate of the next state can be updated recursively [30], [40].

For mobility estimation with heterogeneous sensing, the system is typically nonlinear; therefore, a nonlinear state-space representation is used that more accurately captures sensor interactions and vehicle motion behavior:

$$\begin{aligned} x_{k+1} &= f(x_k) + w_k \\ z_k &= g(x_k) + \eta_k \end{aligned} \quad (3)$$

where $f(x_k)$ and $g(x_k)$ represent the nonlinear vehicle-motion function and measurement function. These functions are required because the vehicle motion depends on nonlinear trigonometric relationships among position, heading, speed, and steering direction. Therefore, standard linear Kalman filtering is not sufficient, and nonlinear filters such as EKF, UKF, PF, and IMM-EKF are used in this study.

C. VEHICLE KINEMATIC MODEL (BICYCLE MODEL)

The simulated vehicle with steerable wheels used in this study is based on the model proposed in [40]. This vehicle is a four-wheeled car-like structure, featuring front wheels that rotate about the vertical axis for steering. Fig 2 shows the coordinate frame, the implemented four-wheel planar vehicle, and its corresponding configuration. A comprehensive description of the vehicle dynamic model is available in [40].

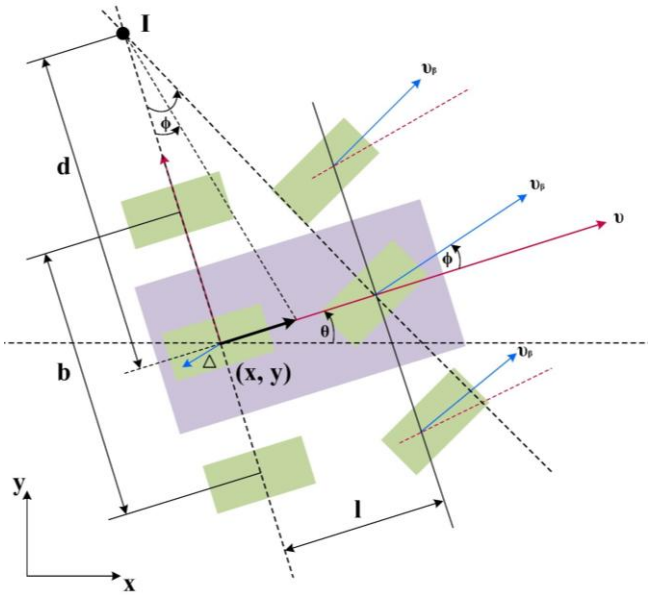

Fig 2. Four-Wheel Vehicle's Kinematic Model (coordinate frame and configuration), adapted from [40]

The kinematic model for straight-motion or no-maneuvering conditions is represented by the following transition equations between instants k and $k+1$ in a bicycle model, describing the evolution of the vehicle states over time under straight-motion conditions without turning effects.

$$\begin{aligned} x_{k+1} &= x_k + t_s v_k cos\,(\theta_k + \phi_k + s_k) \\ &\quad + \frac{1}{2} t_s^2 \dot{v}_k cos\,(\theta_k + \phi_k + s_k) \\ &\quad - \frac{1}{2} t_s^2 v_k \dot{\theta}_k sin\,(\theta_k + \phi_k + s_k) \\ y_{k+1} &= y_k + t_s v_k sin\,(\theta_k + \phi_k + s_k) \\ &\quad + \frac{1}{2} t_s^2 \dot{v}_k sin\,(\theta_k + \phi_k + s_k) \\ &\quad + \frac{1}{2} t_s^2 v_k \dot{\theta}_k\, cos(\theta_k + \phi_k + s_k) \end{aligned} \quad (4)$$

$$\theta_{k+1} = \theta_k + t_s \dot{\theta}_k + \frac{1}{2} t_s^2 \ddot{\theta}_k$$

$$\dot{\theta}_{k+1} = \dot{\theta}_k + t_s \ddot{\theta}_k$$

$$v_{k+1} = v_k + t_s \dot{v}_k$$

$$\phi_{k+1} = \phi_k + t_s \dot{\phi}_k$$

$$s_{k+1} = s_k + t_s \dot{s}_k$$

The corresponding state vector contains seven state variables:

$$x_k = [x_k, y_k, \theta_k, \dot{\theta}_k, v_k, \phi_k, s_k]^\top \quad (5)$$

In this model, x_k and y_k represent the planar position of the vehicle center of mass along the x and y axes, respectively. θ is the vehicle orientation, v is the linear speed, and ϕ represents the wheel/speed direction angle in the vehicle reference frame. The term s_k is an angle-offset correction that influences deviation from the desired course. As defined in the adopted model, s_k is included as a state variable in the referenced model, but its detailed behavior is not fully specified and may be excluded in simulation when appropriate. The intersection point I is known as the instantaneous center of rotation, and the vehicle geometry is defined by b, l, and Δ.

The discrete motion model (4) can also be written in compact nonlinear state-space form:

$$x_{k+1} = f(x_k) + G(x_k)\mathrm{v}_k \quad (6)$$

In the context of the model, the transition matrix function is denoted by f, and G represents the noise gain matrix, which is dependent on the state at time k. The vehicle state vector is represented by x, and the noise vector is denoted as v, defined by $vk \sim N(0, Q_k)$.

D. PROCESS AND MEASUREMENT NOISE MODELS

In the proposed state-space formulation, uncertainty appears in two forms: process noise and measurement noise. Process noise represents uncertainty in the vehicle motion model, such as unmodeled acceleration, small steering variations, and approximation errors in the kinematic model. Measurement noise represents uncertainty in the sensor readings obtained from GPS, IMU, odometry, and BLE-based measurements. Following the adopted vehicle model, the process noise vector is defined as:

$$\mathrm{v}_k = [\ddot{\theta}_k, \dot{v}_k, \dot{\phi}_k, \dot{s}_k]^\top \quad (7)$$

Q_k denotes the covariance matrix of the process noise. In the simulation, it is assumed to remain constant in both time and structure, as expressed in (8).

$$Q_k = [\sigma_x^2, \sigma_y^2, \sigma_\theta^2, \sigma_{\dot{\theta}}^2, \sigma_v^2, \sigma_\phi^2, \sigma_s^2]\boldsymbol{I}_7 \quad (8)$$

The observation vector is defined in (9).

$$z_k = Hx_k + w_k \quad (9)$$

where z is the observation vector containing the system measurements at time step k.

$$z_k = \begin{bmatrix} x_k^{GPS}, y_k^{GPS}, x_k^{IMU}, y_k^{IMU}, \\ \theta_k^{IMU}, \dot{\theta}_k^{odo}, v_k^{odo}, \phi_k^{odo}, v_k^{IMU} \end{bmatrix}^\top \quad (10)$$

The measurement noise w is assumed to follow a zero-mean Gaussian distribution, denoted as $wk \sim N(0, R_k)$. The sensor noise covariance matrix is represented by R_k (11).

$$\begin{aligned} R_k = \; & [\sigma_{x_{GPS}}^2, \sigma_{y_{GPS}}^2, \sigma_{x_{IMU}}^2, \\ & \sigma_{y_{IMU}}^2, \sigma_{\theta_{IMU}}^2, \sigma_{\dot{\theta}_{odo}}^2, \\ & \sigma_{v_{odo}}^2, \sigma_{\phi_{odo}}^2, \sigma_{v_{IMU}}^2]\boldsymbol{I}_9 \end{aligned} \quad (11)$$

The state vector x and the observation vector z are related through a constant linear measurement matrix H.

E. CURVED MANEUVERING EXTENSION

To represent curved maneuvering, the state is extended by including the steering-angle rate term. The curved-motion state vector is defined as:

$$x_k = [x_k, y_k, \theta_k, \dot{\theta}_k, v_k, \phi_k, \dot{\phi}_k, s_k]^\top \quad (12)$$

and the corresponding process-noise vector becomes:

$$\mathrm{v}_k = [\ddot{\theta}_k, \dot{v}_k, \ddot{\phi}_k, \dot{s}_k]^\top \quad (13)$$

This extended formulation supports motion with higher curvature and greater acceleration variation. It is

used alongside the straight-motion model when applying IMM-EKF in later stages of the methodology.

F. FILTERING METHODS IMPLEMENTED

1) Extended Kalman Filter

To estimate mobility parameters under nonlinear vehicle dynamics and heterogeneous sensing, this study implements and compares four nonlinear estimation approaches: EKF, UKF, PF, and an IMM-EKF. These methods are selected because the indoor-outdoor positioning problem involves nonlinear state evolution and measurements whose quality varies across environments (e.g., noisy GNSS outdoors and radio variability indoors).

The EKF is a widely used nonlinear extension of the Kalman filter. It uses a recursive predict-update structure and handles nonlinearity by linearizing the motion and measurement models around the current estimate. In this work, the EKF provides a computationally efficient baseline suitable for real-time estimation. Fig 3 shows the EKF-based estimated position over time for the simulated vehicle trajectory.

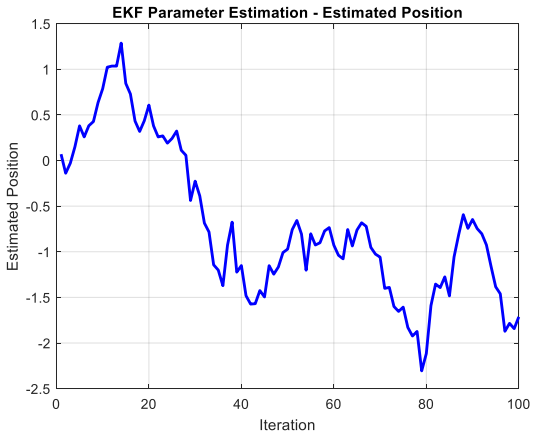

Fig 3. Estimated Position Over Time

2) Unscented Kalman Filter

The UKF is designed for nonlinear systems without explicit linearization. Instead of computing Jacobians, the UKF uses the unscented transform, propagating a set of sigma points through nonlinear functions to better capture the transformed mean and covariance. This often improves estimation accuracy when nonlinearities are stronger. In the UKF implementation used in this study, the parameters are set to $\alpha = 1, \kappa = 0$, and $\beta = 2$. Fig 4 presents the parameter-estimation results obtained using the UKF.

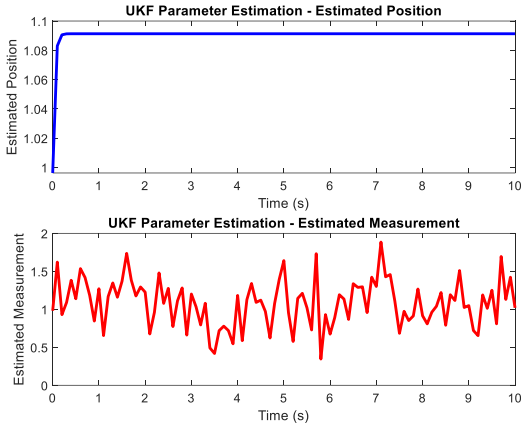

Fig 4. UKF Parameter Estimation Results

3) Particle Filter

PF is a sampling-based Bayesian estimator designed for nonlinear and non-Gaussian problems. It represents the state distribution with weighted particles, updates them using measurements, and applies resampling to emphasize the most likely states. In this study, PF handles uncertainty and measurement variability in indoor-outdoor vehicle estimation. Fig 5 shows the 1D mobility-parameter estimation performance of the PF.

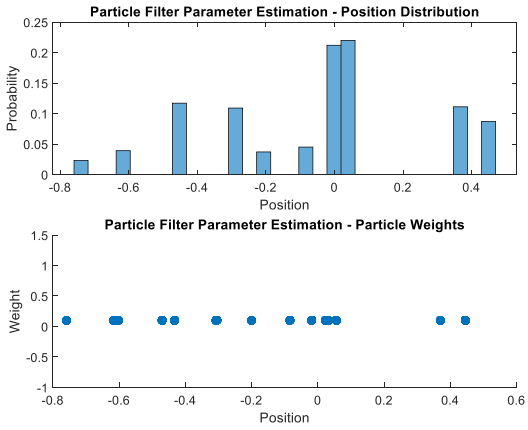

Fig 5. Particle Filter for 1D Mobility Parameter Estimation

To handle changes vehicle maneuvering behavior, this study also implements an IMM-EKF. The IMM-EKF runs two EKFs in parallel throughout the trajectory:

- A model optimized for rectilinear (straight) maneuverability, and
- A model optimized for curvilinear (curved) maneuverability.

During filtering, the IMM-EKF evaluates the probability of each motion model and generates state estimates from the most likely one. This matches the simulation design, where motion

behavior changes during indoor-outdoor transitions.

G. OBSERVABILITY ANALYSIS APPROACH

Sensors commonly operate at varying sampling frequencies, introducing the possibility of information loss during measurements due to sensor faults. For instance, in urban environments utilizing GPS sensors, entry into an urban canyon formed by towering buildings may lead to a temporary loss of GPS sensor measurements. Multisensory fusion systems may involve filters with disparate sampling rates, contributing to potential challenges. During the implementation of Kalman filtering, the temporary disappearance of a measurement, even if brief, can instigate instability in the "Riccati" equation, potentially resulting in complete detuning of the filter [41]. Fig 6 shows the structure of the proposed simulator used for position estimation and observability analysis.

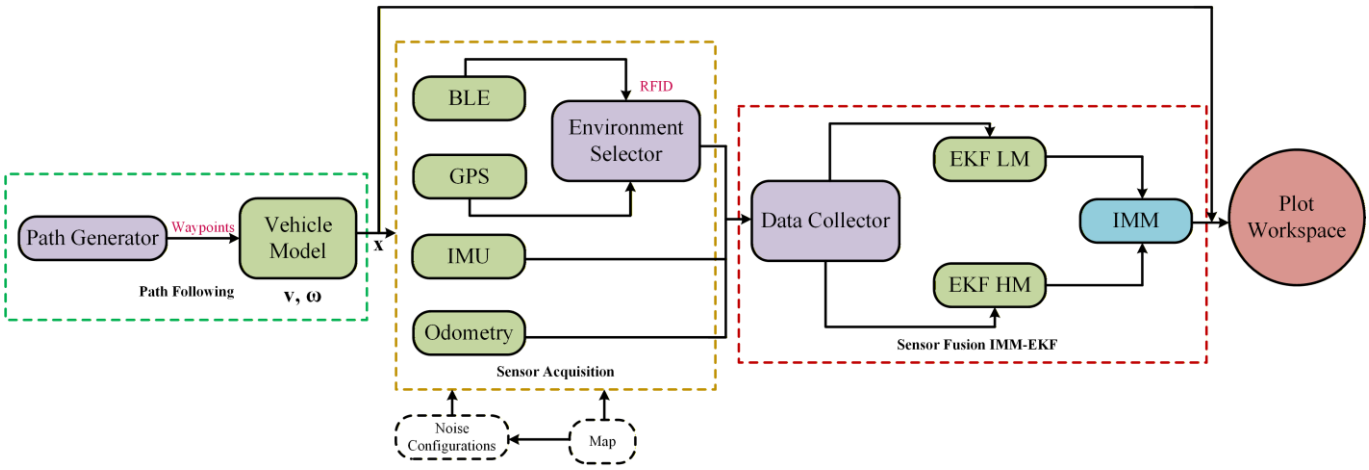

Fig 6. Structure of the Proposed Simulator for Vehicle Position Estimation

In essence, an observable system encompasses all the necessary information for making estimates with limited error. A system is deemed non-observable when certain elements of the state vector at time k cannot be determined from the observations (outputs) and recorded system inputs.

For linear systems with constant parameters, observability is characterized by the rank condition. Specifically, a linear system is observable if and only if the matrix range $[HHA \ldots HA^{n-1}]$ equals the n dimension of the state space. The space extending through the functions $H\,x, H\,Ax, \ldots, HA^{n-1}x$ represents the observation space of the system. If the spread space of the elements of $\mathcal{O} \cdot \mathrm{d}\mathcal{O}(x)$ evaluated in x has a rank equal to n for any x, then the system is said to satisfy the observability condition. Observability is further determined by whether the observability matrix, denoted as M_{obs}, is of full rank. The observability matrix M_{obs} is defined as:

$$M_{obs} = \begin{bmatrix} H \\ HA \\ \vdots \\ HA^{i} \\ \vdots \\ HA^{n-1} \end{bmatrix} \tag{14}$$

In systems characterized by a state vector denoted as x with a dimensionality of m, observability is confirmed when the observability matrix M_{obs} achieves a rank equal to m. This condition indicates that the linear system exhibits n linearly independent columns [42].

For nonlinear systems, the classical linear observability test cannot be applied directly [43]. In this work, observability is approximated using local linearization, consistent with the study's EKF-based approach. The key idea is to replace the linear transition matrix A with the Jacobian of the nonlinear transition function evaluated at the current operating state [44]. To approximate the observability of a nonlinear system, one can employ local linearization of such systems. For instance, the Extended Kalman Filter (EKF) linearizes nonlinear systems at a state x_k and subsequently applies the linear Kalman filter using the linearized model. The Jacobians obtained through the linearization of the EKF can serve as substitutes for the matrices A and H in the non-linear system. In the context of the four-wheeled car estimation problem proposed, it is assumed that $u \equiv 0$ is a universal entry. The Jacobian $\{\xi 1, \xi 2, \ldots, \xi n\} = \{h, L_f h, \ldots, L_f^{n-1} h\}$ with respect to x has an equal rank of n at the point x_0. The observability criteria established for linear systems cannot be directly applied to non-linear systems. To

address this, substitutions can be made using truncated Taylor series, enabling the linearization of the system. One approach is to incorporate the Jacobian of the transition function f and, if required, the function H into the observability matrix (14). The Jacobian of the function f is assessed at $x = \hat{x}(k + 1/k)$ and serves as a replacement for the transition matrix A. The resulting observability matrix becomes:

$$M_{obs} = \begin{bmatrix} H \\ HF(x,k) \\ \vdots \\ HF(x,k)^{i} \\ \vdots \\ HF(x,k)^{n-1} \end{bmatrix} \quad (15)$$

where the Jacobian is defined as:

$$F(x,k) = \frac{\partial f(x,k)}{\partial x}\Big|_{x=x_k} \quad (16)$$

Because the Jacobian depends on the state, a single observability matrix that is valid for all operating conditions is generally not available. Therefore, observability is evaluated locally at representative states along the trajectory, using the linearized model produced during EKF operation [45]. This approach provides a practical way to determine whether the system remains observable under different sensor-availability conditions during indoor-outdoor transitions.

H. Simulation Design and BLE RSS Model

To evaluate nonlinear filtering performance and observability for indoor-outdoor positioning, a simulator was developed for a four-wheel vehicle traveling from one indoor environment to another through an outdoor segment. The simulator reproduces vehicle motion based on a predefined trajectory generated by the vehicle control inputs: linear velocity $v$and angular velocity $\omega = \dot{\phi}$. The sensing configuration used in this study includes GPS/SBAS (GNSS), BLE-based measurements, IMU inertial sensing, and odometry. In addition, the simulation allows variations in GPS signal quality to represent conditions such as urban canyon effects or artificial interference along the route [37], [46].

In the simulation stage where BLE is used for indoor position estimation, the locations of BLE transmitters are assumed known. This study adopts a reference distance of $d_0 = 1$ m under line-of-sight conditions, with an average transmission power of -41.5 dBm. The propagation loss coefficient is set to $\alpha = 2$ for a carrier frequency of 2.4 GHz under line-of-sight assumptions. The received signal strength (RSS) from transmitter i at distance d_k is modeled as:

$$RSS^{i}_{d_k} = RSS^{i}_{d_0} + 10\alpha log_{10}(d_k) + \eta_{BLE} + q_{BLE} \quad (17)$$

where η_{BLE} represents multipath-induced noise and is modeled as Gaussian, $\eta_{BLE} \sim \mathcal{N}(0, \sigma^2_{BLE})$. The term q_{BLE} represents quantization noise due to the discrete RSS representation in the BLE protocol and is modeled as a uniform random variable with magnitude linked to the quantizer least significant bit (LSB), consistent with the study description.

IV. Results and Discussion

A. Simulation Scenario and Visualization

The simulator produces an animation of a four-wheel vehicle traveling from Building A to Building B, with an outdoor segment between the two indoor environments. The simulation environment allows the definition of the positions and sizes of the buildings as well as the route followed by the vehicle. To reflect realistic outdoor challenges, the simulator also supports controlled variation of GNSS/GPS measurement quality, enabling scenarios that resemble urban-canyon effects or artificial interference, in which GPS observations become noisy or temporarily degraded [46]. Fig 7 shows a realization of the simulation environment and animation, including the vehicle trajectory and building layout.

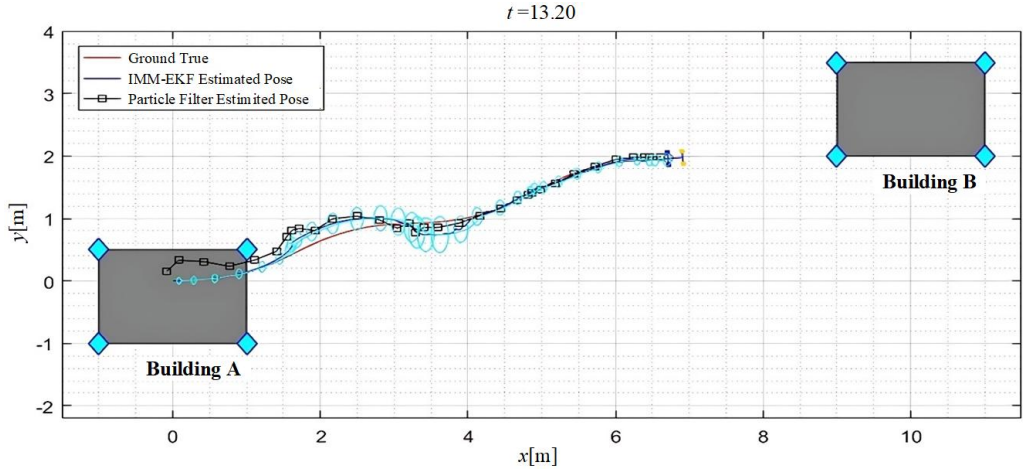

Fig 7. Simulation Environment and Vehicle Trajectory Visualization

The visualization shows the moving vehicle together with the building layout and trajectory. It includes the ground-truth path and the estimated trajectories produced by the fusion filters. In this study, the IMM-EKF and Particle Filter estimates are displayed with the true trajectory using the MATLAB Robotics Toolbox. This gives an intuitive view of estimator performance during the indoor-outdoor transition and shows the impact of sensor fusion under changing measurement quality.

B. FILTER PERFORMANCE COMPARISON

Filter performance was assessed by comparing the estimated vehicle trajectory with the ground-truth trajectory over the complete indoor-outdoor transition. The same simulated sensor inputs, including GNSS/GPS with variable quality, BLE RSS, IMU, and odometry, were used for all evaluated filters. For each filter, the position estimation errors in the x and y directions were examined, and the Euclidean position error was used in the trajectory-error visualization to show the overall deviation from the ground-truth path. The statistical comparison in

Tbl 1 focuses on the component-wise position errors and heading error, which provide a consistent basis for comparing the bias and dispersion of IMM-EKF, UKF, and PF.

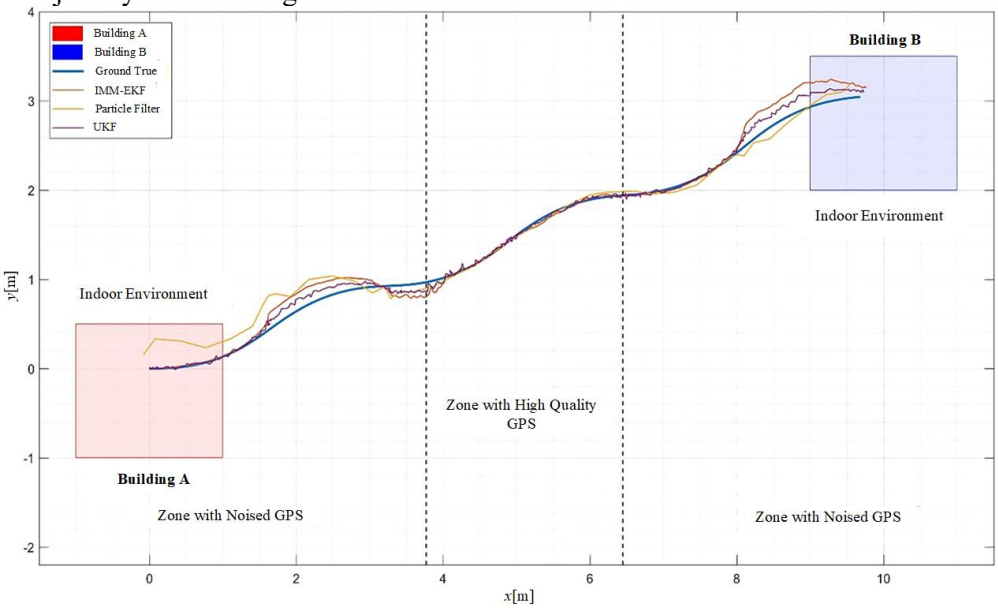

Fig 8. Trajectory Comparison of Multi-Sensor Fusion Methods: IMM-EKF, UKF, and Particle Filter

As shown in Fig 8, the estimation errors and their distributions enable direct comparison of the filters under identical transition conditions. The error histograms are approximately Gaussian, supporting statistical evaluation of estimator behavior. Overall, the results show that multi-sensor fusion provides stable trajectory tracking during indoor-outdoor transitions, while the three filters exhibit different error characteristics along the trajectory.

C. STATISTICAL PERFORMANCE SUMMARY

To quantitatively evaluate the implemented filters, the estimation errors were calculated with respect to the ground-truth vehicle trajectory over the complete indoor-outdoor transition. Let $\hat{x}_k$, $\hat{y}_k$, and $\hat{\theta}_k$ denote the estimated position and heading at sample k, while x_k^{true}, y_k^{true}, and θ_k^{true} denote the corresponding ground-truth values. The position errors are defined as $e_{x,k} = \hat{x}_k - x_k^{true}$ and $e_{y,k} = \hat{y}_k - y_k^{true}$, and the heading error is defined as $e_{\theta,k} = \hat{\theta}_k - \theta_k^{true}$. The mean error μ represents the average estimation bias, while the standard deviation σ represents the dispersion of the error around its mean value. Position-related metrics are reported in meters, and heading-related metrics are reported in degrees.

Tbl 1. Statistical Summary of Position and Heading Estimation Errors for the Evaluated Filters

Filter	μ_x (m)	σ_x (m)	μ_y (m)	σ_y (m)	μ_θ (°)	σ_θ (°)
IMM-EKF	0.40	2.51	0.14	3.11	0.15	1.56
UKF	0.31	3.40	0.44	3.66	0.06	1.49
PF	1.2	4.2	0.26	3.14	0.04	1.64

As shown in

Tbl 1, IMM-EKF achieved the most consistent overall position-estimation performance in the tested scenario. Although UKF produced a slightly lower mean error in the x direction, IMM-EKF provided lower dispersion in the position estimates, with $\sigma_x = 2.51\,\text{m}$ and $\sigma_y = 3.11\,\text{m}$. In comparison, UKF produced $\sigma_x = 3.40\,\text{m}$ and $\sigma_y = 3.66\,\text{m}$, while PF produced $\sigma_x = 4.20\,\text{m}$ and $\sigma_y = 3.14\,\text{m}$. These results indicate that IMM-EKF provides more stable trajectory estimation during the indoor-outdoor transition.

D. OBSERVABILITY RANK RESULTS

Observability was evaluated using the EKF-based local linearization approach described in Section III-G. The analysis was performed for the seven-state vehicle model defined in (5); therefore, the full state dimension is $n = 7$. A sensor configuration is considered fully locally observable when the observability matrix satisfies $rank(\mathcal{O}) = 7$. If $rank(\mathcal{O}) < 7$, the sensor configuration is considered partially observable because the available measurements are not sufficient to reconstruct the complete vehicle state.

Tbl 2. Observability Rank Results for Different Sensor Availability Conditions

Sensor set	Rank ($\mathcal{O}$)	Full state dimension n	Observability status
GPS	5	7	Partially observable
Odometer	3	7	Partially observable
IMU	7	7	Fully observable
IMU + Odometer	5	7	Partially observable
GPS + Odometer	5	7	Partially observable
GPS + IMU	7	7	Fully observable
All sensors	7	7	Fully observable

The results in Tbl 2 show that full local observability is achieved when the observability rank reaches 7. IMU-only, GPS+IMU, and the full sensor configuration achieve full observability in the adopted seven-state model. In contrast, GPS-only, odometer-only, IMU+odometer, and GPS+odometer configurations remain partially observable because their ranks are lower than the full state dimension. These results show that IMU measurements play a critical role in maintaining full-state estimation during indoor-outdoor transitions, especially when GNSS/GPS measurements are degraded or unavailable.

V. CONCLUSION

This study presented a simulation-based framework for mobility parameter estimation to enable seamless indoor–outdoor positioning of a four-wheel vehicle using heterogeneous sensing, including GNSS/GPS, BLE RSS, IMU, and odometry. A nonlinear state-space vehicle model was used to implement and compare the EKF, UKF, PF, and IMM-EKF. The IMM-EKF combined rectilinear and curvilinear motion models to handle changes in vehicle maneuvering behavior. The results show that multi-sensor fusion supports accurate and stable trajectory estimation under time-varying and noisy sensing conditions, with the IMM-EKF providing the most consistent overall performance in the tested transition scenario. The EKF-based local observability analysis further indicates that full-state observability is achieved when IMU measurements are available in the sensing configuration, including the GPS+IMU case. In contrast, reduced sensor subsets, such as GPS-only and odometer-only configurations, are not fully observable. These findings underscore the importance of observability-aware sensor-fusion design for robust indoor-outdoor vehicle positioning.

REFERENCES

[1] T. G. Hailu, X. Guo, and H. Si, “Indoor Positioning Systems as Critical Infrastructure: An Assessment for Enhanced Location-Based Services,” *Sensors*, vol. 25, no. 16, p. 4914, Aug. 2025.

[2] T. Aziz and I. Koo, “A Comprehensive Review of Indoor Localization Techniques and Applications in Various Sectors,” *Applied Sciences*, vol. 15, no. 3, p. 1544, Feb. 2025.

[3] P. S. Farahsari, A. Farahzadi, J. Rezazadeh, and A. Bagheri, “A Survey on Indoor Positioning Systems for IoT-Based Applications,” *IEEE Internet Things J.*, vol. 9, no. 10, pp. 7680–7699, May 2022.

[4] S. Kumar, K. Sakagami, and H. P. Lee, “Beyond Sustainability: The Role of Regenerative Design in Optimizing Indoor

Environmental Quality," *Sustainability 2025, Vol. 17, Page 2342*, vol. 17, no. 6, p. 2342, Mar. 2025.

[5] Y. Xie, M. E. R. Ekra, T. Gu, and X. Wang, "A Research on Positioning Algorithm Based on RPCA in Sparse Fingerprint Environment," *International Journal of Informatics, Information System and Computer Engineering (INJIISCOM)*, vol. 6, no. 2, pp. 225–245, Feb. 2025.

[6] M. Shahraki, A. Elamin, and A. El-Rabbany, "Indoor UAV 3D Localization Using 5G CSI Fingerprinting," *ISPRS Int. J. Geoinf.*, vol. 15, no. 1, p. 24, Jan. 2026.

[7] G. Guo, R. Chen, K. Yan, P. Li, L. Yuan, and L. Chen, "Multichannel and Multi-RSS Based BLE Range Estimation for Indoor Tracking of Commercial Smartphones," *IEEE Sens. J.*, vol. 23, no. 24, pp. 30728–30738, Dec. 2023.

[8] J. Liu, Z. Yang, S. Zlatanova, S. Li, and B. Yu, "Indoor Localization Methods for Smartphones with Multi-Source Sensors Fusion: Tasks, Challenges, Strategies, and Perspectives," *Sensors*, vol. 25, no. 6, p. 1806, Mar. 2025.

[9] A. Takanose, K. Kondo, Y. Hoda, J. Meguro, and K. Takeda, "Localization System for Vehicle Navigation Based on GNSS/IMU Using Time-Series Optimization with Road Gradient Constrain," *Journal of Robotics and Mechatronics*, vol. 35, no. 2, pp. 387–397, Apr. 2023.

[10] X. Wang, T. Chen, R. Wang, J. Lu, and G. Dou, "Review of State Estimation Methods for Autonomous Ground Vehicles: Perspectives on Estimation Objects, Vehicle Characteristics, and Key Algorithms," *Sensors*, vol. 25, no. 13, p. 3927, Jun. 2025.

[11] S. Wang and N. S. Ahmad, "A Comprehensive Review on Sensor Fusion Techniques for Localization of a Dynamic Target in GPS-Denied Environments," *IEEE Access*, vol. 13, pp. 2252–2285, Dec. 2024.

[12] G. Revach, N. Shlezinger, X. Ni, A. L. Escoriza, R. J. G. Van Sloun, and Y. C. Eldar, "KalmanNet: Neural Network Aided Kalman Filtering for Partially Known Dynamics," *IEEE Transactions on Signal Processing*, vol. 70, pp. 1532–1547, Mar. 2022.

[13] K. György, A. Kelemen, and L. Dávid, "Unscented Kalman Filters and Particle Filter Methods for Nonlinear State Estimation," *Procedia Technology*, vol. 12, pp. 65–74, Jan. 2014.

[14] H. Fang, N. Tian, Y. Wang, M. Zhou, and M. A. Haile, "Nonlinear Bayesian estimation: From Kalman filtering to a broader horizon," *IEEE/CAA Journal of Automatica Sinica*, vol. 5, no. 2, pp. 401–417, Mar. 2018.

[15] K. Wang, L. Wu, Y. Ben, Q. Li, C. Lv, and L. Hou, "Robust Factor Graph Optimization for GNSS/INS Tightly Coupled Integration: A Flexible Strategy for Urban Navigation Resilience," *IEEE Sens. J.*, vol. 25, no. 15, pp. 29296–29309, Jul. 2025.

[16] T. Kabir, "Digital Twin–Enabled Optimization of Electrical, Instrumentation, And Control Architectures In Smart Manufacturing And Utility-Scale Systems," *International Journal of Scientific Interdisciplinary Research*, vol. 6, no. 1, pp. 404–451, Jun. 2025.

[17] J. Wu, J. Jiang, Y. Tang, and J. Liu, "Gaussian–Student's t Mixture Distribution-Based Robust Kalman Filter for Global Navigation Satellite System/Inertial Navigation System/Odometer Data Fusion," *Remote Sens. (Basel).*, vol. 16, no. 24, p. 4716, Dec. 2024.

[18] T. Devos, M. Kirchner, J. Croes, W. Desmet, and F. Naets, "Sensor Selection and State Estimation for Unobservable and Non-Linear System Models," *Sensors*, vol. 21, no. 22, p. 7492, Nov. 2021.

[19] M. Stefanoni, I. Kovács, P. Sarcevic, and Á. Odry, "A Survey on the Main Techniques Adopted in Indoor and Outdoor Localization," *Electronics (Basel).*, vol. 14, no. 10, p. 2069, May 2025.

[20] A. Michler, P. Schwarzbach, J. Ninnemann, M. Ammad, and O. Michler, "An empirical assessment of indoor-outdoor localization based on signals of opportunity from multiple systems," *2025 IEEE/ION Position, Location and Navigation Symposium, PLANS 2025*, pp. 948–959, Jun. 2025.

[21] K. Song, J. Li, M. Ren, and S. Liu, "Indoor and Outdoor Fusion Positioning System Based on UWB/GNSS/IMU Multi-Sensor Technology," in *ACM International Conference Proceeding Series*, 2024, vol. 24, pp. 48–54.

[22] M. E. R. Ekra, T. Mahmud, I. Hossain, R. Haque, M. Masum, and H. Maruf, "Wi-Fi Indoor Location Method based on Improved Fingerprint Technique," *European Journal of Electrical Engineering and Computer Science*, vol. 9, no. 2, pp. 33–39, Apr. 2025.

[23] C. S. Mouhammad, A. Allam, M. Abdel-Raouf, E. Shenouda, and M. Elsabrouty, "BLE Indoor Localization based on Improved RSSI and Trilateration," in *Proceedings of the International Japan-Africa Conference on Electronics, Communications and Computations, JAC-ECC 2019*, 2019, pp. 17–21.

[24] Y. Qu, M. Yang, J. Zhang, W. Xie, B. Qiang, and J. Chen, "An Outline of Multi-Sensor Fusion Methods for Mobile Agents Indoor Navigation," *Sensors*, vol. 21, no. 5, p. 1605, Feb. 2021.

[25] Y. Yang and B. Huang, "An Energy-Efficient Smartphone Positioning Scheme by Fusing WiFi, GPS and PDR," in *2023 19th International Conference on Mobility, Sensing and Networking (MSN)*, 2023, pp. 64–71.

[26] M. Heshmat, L. Saad Saoud, M. Abujabal, A. Sultan, M. Elmezain, L. Seneviratne, and I. Hussain, "Underwater SLAM Meets Deep Learning: Challenges, Multi-Sensor Integration, and Future Directions," *Sensors*, vol. 25, no. 11, p. 3258, May 2025.

[27] S. Wang, P. Dai, T. Xu, W. Nie, Y. Cong, F. Gao, and J. Xing, "Application of variational Bayesian-based cubature information filter for UWB/INS tightly coupled positioning system," *Meas. Sci. Technol.*, vol. 36, no. 4, p. 046302, Mar. 2025.

[28] M. Stefanoni, I. Kovacs, R. Pesti, D. Csik, P. Sarcevic, and A. Odry, "Enhancing 2D Localization Accuracy for Differential Wheeled Robots: A Fusion of Odometry, Magnetometers, and Absolute Positioning Systems," in *SISY 2025 - IEEE 23rd International Symposium on Intelligent Systems and Informatics, Proceedings*, 2025, pp. 393–398.

[29] S. Särkkä and L. Svensson, *Bayesian filtering and smoothing*, 2nd ed. Cambridge university press, 2023.

[30] E. Safikou and G. M. Bollas, "Inferential Sensors in an Extended Kalman Filter for Fault Estimation," in *IFAC-PapersOnLine*, 2024, vol. 58, no. 14, pp. 634–639.

[31] F. Gustafsson, *Statistical sensor fusion*, 1st ed. Lund: Studentlitteratur, 2010.

[32] Z. Li, Q. Meng, Z. Shen, L. Wang, L. Li, and H. Jia, "Resilient Factor Graph-Based GNSS/IMU/Vision/Odo Integrated Navigation Scheme Enhanced by Noise Approximate Gaussian Estimation in Challenging Environments," *Remote Sens. (Basel).*, vol. 16, no. 12, p. 2176, Jun. 2024.

[33] P. Wang, W. Li, and X. Diao, "Indoor and Outdoor Seamless Positioning Technology Based on Artificial Intelligence and Intelligent Switching Algorithm," *Wirel. Commun. Mob. Comput.*, vol. 2023, no. 1, p. 7075834, Jan. 2023.

[34] B. Zhou, H. Fang, and J. Xu, "UWB-IMU-Odometer Fusion Localization Scheme: Observability Analysis and Experiments," *IEEE Sens. J.*, vol. 23, no. 3, pp. 2550–2564, Feb. 2023.

[35] P. Bauer, "Sensor Bias Ambiguity in GNSS-IMU Pose Estimation and Its Solution," *ASME Letters in Dynamic Systems and Control*, vol. 5, no. 4, p. 041008, Oct. 2025.

[36] P. Bahl and V. N. Padmanabhan, "RADAR: An in-building RF-based user location and tracking system," in *Proceedings - IEEE INFOCOM*, 2000, vol. 2, pp. 775–784.

[37] P. Corke, W. Jachimczyk, and R. Pillat, *Robotics, Vision and Control*, 2nd ed. Cham: Springer International Publishing, 2023.

[38] M. Teran, J. Aranda, H. Carrillo, D. Mendez, and C. Parra, "IoT-based system for indoor location using bluetooth low energy," in *2017 IEEE Colombian Conference on Communications and Computing, COLCOM 2017 - Proceedings*, 2017, pp. 1–6.

[39] F. Zafari, A. Gkelias, and K. K. Leung, "A Survey of Indoor Localization Systems and Technologies," *IEEE Communications Surveys and Tutorials*, vol. 21, no. 3, pp. 2568–2599, Apr. 2019.

[40] R. Toledo-Moreo, M. A. Zamora-Izquierdo, B. Úbeda-Miñarro, and A. F. Gómez-Skarmeta, "High-integrity IMM-EKF-based road vehicle navigation with low-cost GPS/SBAS/INS," *IEEE Transactions on Intelligent Transportation Systems*, vol. 8, no. 3, pp. 491–511, Sep. 2007.

[41] Y. Bar-Shalom, X. -Rong Li, and T. Kirubarajan, *Estimation with Applications to Tracking and Navigation*, 1st ed. Wiley, 2002.

[42] K. Ogata, *Modern Control Engineering*, 5th ed. Prentice Hall, 2010.

[43] R. Hermann and A. J. Krener, "Nonlinear Controllability and Observability," *IEEE Trans. Automat. Contr.*, vol. 22, no. 5, pp. 728–740, Oct. 1977.

[44] V. K. Dertimanis, E. N. Chatzi, S. Eftekhar Azam, and C. Papadimitriou, "Input-state-parameter estimation of structural systems from limited output information," *Mech. Syst. Signal Process.*, vol. 126, pp. 711–746, Jul. 2019.

[45] A. Martinelli, "State estimation based on the concept of continuous symmetry and observability analysis: The case of calibration," *IEEE Transactions on Robotics*, vol. 27, no. 2, pp. 239–255, Mar. 2011.

[46] J. Zidan, E. I. Adegoke, E. Kampert, S. A. Birrell, C. R. Ford, and M. D. Higgins, "GNSS Vulnerabilities and Existing Solutions: A Review of the Literature," *IEEE Access*, vol. 9, pp. 153960–153976, Feb. 2020.

AUTHORS BIOGRAPHY AND CONTRIBUTIONS

Md Emadur Rahman Ekra, received the B.S. degree in Electronic and Information Engineering from Nanjing University of Information Science & Technology (NUIST), Nanjing, China, in 2023, and the M.S. degree in Information and Communication Engineering from the School of Electronic and Information Engineering, Nanjing University of Information Science & Technology (NUIST), Nanjing, China, in 2025. He is currently engaged in research in the field of Electronic and Information engineering. His main research interests include wireless sensor networks, wireless positioning, autonomous vehicle control, cooperative control, networked control systems, and IoT-enabled smart systems. In this article, he contributed to conceptualization, methodology, system modeling, simulation, analysis, visualization, and manuscript writing.

Md Nadim Hosain, received the B.S. degree in Electrical and Automation Engineering from Nanjing University of Information Science & Technology (NUIST), Nanjing, China, in 2025 and is currently pursuing the M.S. degree in Information and Communication Engineering from the School of Electronic and Information Engineering, Nanjing University of Information Science and Technology (NUIST), Nanjing, China. His main research interests include wireless sensor networks, wireless positioning and IoT. In this article, he contributed to simulation support, result validation, visualization, and manuscript revision.

Md Daud Ibrahim, is currently pursuing the B.S. degree in Electronic and Information Engineering at Nanjing University of Information Science & Technology (NUIST), Nanjing, China. His main research interests include wireless sensor networks and IoT. In this article, he contributed to literature review, simulation assistance, result validation, visualization, and manuscript review.

Md Imran Hossain, is currently pursuing the B.S. degree in Electronic and Information Engineering at Nanjing University of Information Science & Technology (NUIST), Nanjing, China. His main research interests include wireless positioning and application of IoT. In this article, he contributed to experimental support, result checking, visualization, and manuscript revision.

Md Belayet Hossain Babla, is currently pursuing the B.S. degree in Electronic and Information Engineering at Nanjing University of Information Science & Technology (NUIST), Nanjing, China. His main research interests include wireless sensor networks and wireless positioning. In this article, he contributed to literature support, simulation assistance, visualization, and manuscript review.